Novel Dendritic Chromophores for Electro-optics: Influence of Binding Mode and Attachment Flexibility on Electro-optic Behavior

Philip A. Sullivan,*,† Andrew J. P. Akelaitis,*,† Sang Kyu Lee,‡ Genette McGrew,† Susan K. Lee,† Dong Hoon Choi,‡ and Larry R. Dalton*,†

Department of Chemistry, Box 351700, University of Washington, Seattle Washington 98105, and Department of Chemistry, Korea University, Seoul 136-701, Korea

Received August 4, 2005. Revised Manuscript Received November 7, 2005

Four dendritic electro-optic (EO) chromophores were designed, prepared, and evaluated to explore the effects on EO behavior of end-on relative to side-on chromophore attachment geometry as well as differing chromophore-to-dendrimer core tether groups. Composite samples of APC and dendritic chromophores were found to exhibit considerably more thermally stable EO properties as compared to samples of the corresponding isolated chromophore. Side-on type binding geometry was found most thermally stable, requiring larger thermal activation energies to induce dipole randomization. Incorporation of a long, flexible chromophore−core tether group greatly enhanced average EO coefficients of the dendritic systems.

Introduction

Organic materials exhibiting large electro-optic (EO) response (r_{33}) have drawn considerable attention over the past 2 decades. These materials have extensive potential for use in telecommunications, digital signal processing, phased array radar, THz generation, and many other applications as active materials in photonic microdevices.[1−6] Multichromophore dendritic EO materials were recently introduced as a method for controlling interchromophore electrostatic interactions which are detrimental to the realization of large nonlinear susceptibility ($\chi^{(2)}$) in composite materials. The degree of electric field induced dipolar ordering within a covalently attached chromophore−host matrix, and the resulting macroscale properties, can be expected to be heavily dependent on subtle differences in architectural design.

Organic materials present clear advantages over inorganic materials that have been employed for similar applications. These advantages include lower cost, ease of processing and device integration, and low dielectric constant. Organic materials exhibit potential for highly increased operational bandwidth relative to analogous inorganic-based devices.[7−12] Materials of synthetic origin also present the possibility of application-specific material tailoring. Such applications as those outlined above require thermally robust and photochemically stable materials, which exhibit high macroscopic second-order nonlinear susceptibilities ($\chi^{(2)}$). These requirements have historically presented challenges to the commercialization of organic materials.

To induce high $\chi^{(2)}$ values, electric field poling or molecular assembly techniques must be employed to achieve a bulk acentric (dipolar) ordering of the molecular lattice due to symmetry considerations. The r_{33} value obtained can be directly related to $\chi^{(2)}$ ($-\omega$; ω, 0) of the material by

$$r_{33} = -2\chi^{(2)}{}_{zzz}/(n_z)^4 \tag{1}$$

The magnitude of $\chi^{(2)}$ is directly proportional to the degree of dipolar order produced within the material since the phenomenological parameter is related to molecular parameters by

$$\chi^2{}_{zzz} = NF\beta_{zzz}\langle\cos^3\theta\rangle \tag{2}$$

where N is the number density of active molecules within the medium interacting with EM radiation, F is a local field factor, and $\langle\cos^3\theta\rangle$ represents an order parameter that is essentially a measure of dipolar order within the system. The angle between the chromophore dipole vector and the poling axis is denoted as θ.

Using these relations, it can be shown that the magnitude of r_{33} is directly proportional to the degree of acentric

* Authors to whom correspondence should be addressed. E-mail: psull76@u.washington.edu; aakelai@u.washington.edu; dalton@chem.washington.edu.
† University of Washington.
‡ Korea University.

(1) Dalton, L. R. Nonlinear Optical Polymeric Materials: From Chromophore Design to Commercial Applications. *Advances in Polymer Science*; Springer-Verlag: Berlin, 2002; Vol. 158.
(2) Dalton, L. R.; Harper, A. W.; Ghosen, R.; Steier, W. H.; Ziari, M.; Fetterman, H.; Shi, Y.; Mustacich, R. V.; Jen, A. K.-Y.; Shea, K. J. *Chem. Mater.* **1995**, *7*, 1060−1081.
(3) Samyn, C.; Verbiest, T.; Persoons, A. *Macromol. Rapid Commun.* **2000**, *21*, 1−15.
(4) Shi, Y.; Zhang, C.; Zhang, H.; Betchel, J. H.; Steier, W. H.; Robinson, B.; Dalton L. R. *Science* **2000**, *288*, 119−122.
(5) Sinyukov, A. M.; Leahy, M. R.; Hayden, L. M.; Haller, M.; Luo, J.; Jen, A. K.-Y.; Dalton, L. R. *Appl. Phys. Lett.* **2004**, *85* (24), 5827−5829.
(6) Baehr-Jones, T.; Hochberg, M.; Wang, G.; Lawson, R.; Liao, Y.; Sullivan, P. A.; Dalton, L. R.; Jen, A. K.-Y.; Scherer, A. *Opt. Express* **2005**, *13* (14), 5216−5226.
(7) Lee, M.; Katz, H. E.; Erben, C.; Gill, D. M.; Gopalan, P.; Heber, J. D.; McGee, D. J. *Science* **2002**, *298*, 1401−1403.
(8) Lacroix, P. G. *Chem. Mater.* **2001**, *13*, 3495−3506.
(9) Katti, K. V.; Raghuraman, K.; Pillarsetty, N.; Karra, S. R.; Gulotty, R. J.; Chartier, M. A.; Langhoff, C. A. *Chem. Mater.* **2002**, *14*, 2436−2438.
(10) Facchetti, A.; Abbotto, A.; Beverina, L.; van der Boom, M. E.; Dutta, P.; Evmenenko, G.; Pagani, G. A.; Marks, T. J. *Chem. Mater.* **2003**, *15*, 1064−1072.
(11) Diaz, J. L.; Dobarro, A.; Villacampa, B.; Velasco, D. *Chem. Mater.* **2001**, *13*, 2528−2536.
(12) Chaumel, F.; Jiang, H.; Kakkar, A. *Chem. Mater.* **2001**, *13*, 3389−3395.

10.1021/cm0517420 CCC: $33.50
Published on Web 12/21/2005

chromophore order induced by application of the poling field. The term β_{zzz} represents the molecular first hyperpolarizability tensor component in the direction of the dipole vector of each individual chromophore. Chromophore materials that exhibit large first-order molecular hyperpolarizability (β) values typically also possess high ground state and transitional dipole moments. Large dipole moments contribute to ordering through strong dipole/poling field interactions. However, as chromophore number density increases, these dipoles promote interchromophore electrostatic interactions that compete with external ordering fields, attenuating $\chi^{(2)}$ and macroscopic EO response.[13,14]

Multichromophore dendritic EO materials were recently introduced as a method for forcing chromophore separation through steric interaction, thus reducing detrimental dipole interactions. These materials consist of EO-active, dipolar chromophores covalently bound to form a dendritic structure. This arrangement acts to site-isolate each active unit within the internal free volume created by the dendrimer.[15,16] Site isolation allows each individual chromophore to reorient more independently in response to the external poling field. This reduction of intermolecular electrostatic interactions allows for increased active chromophore number density in the formulation of a composite material, thus enhancing electro-optic response.[17−20] Dendritic encapsulation as well as the use of dendronized side chain EO polymers created by post-functionalization have recently been shown to lead to large EO coefficients and improved material qualities.[21−24] EO materials in which active chromophores are covalently bound also present benefits such as reduction of chromophore−polymer phase separation, enhanced thermal stability of EO effects, and the possibility of using covalent attachment to augment external ordering forces.[25] Covalent chromophore attachment may also be implemented to introduce initial asymmetry or to scaffold innovative architectural design in order to facilitate supramolecular self-assembly. The degree of dipolar ordering within a covalently attached chromophore−host matrix, and the resulting macroscale properties, can be expected to be heavily dependent on subtle differences in architectural design.[26,27] It is thus necessary to explore such dependencies in detail. In particular, in the design of photonic materials based on a dendritic architecture, there exist many fundamentally different possibilities for the covalent attachment of dipolar, high β chromophores to inert matrix building blocks. One important design feature is dipolar orientation with respect to the matrix or dendrimer core. A second is the nature, especially length, flexibility, and polarity, of the spacer group chosen to facilitate chromophore attachment.

To begin exploration of such fundamental architectural design parameters, four dendritic EO chromophores were designed, prepared, and evaluated. A set of two chromophores was first constructed incorporating a succinate diester, chromophore−core tether group. These dendritic chromophores were designed in such a way that they differed only in the dipolar orientation of the active units with respect to the chromophore−core tether group. In one dendritic chromophore the active unit dipoles were oriented normal to the tether group (side-on), and in the other they were oriented parallel to the tether group (end-on). The dendritic chromophores were also compared to the corresponding free chromophore FTC. To investigate the effects of tether group composition, and to more precisely compare thermal relaxation behavior, two additional dendritic chromophores were then designed using information gathered thus far. These dendritic chromophores were again constructed in side-on and end-on fashion but with a longer, more flexible, monoester, chromophore−core tether group derived from a hexanoic acid.

A thiophene-containing, FTC-type chromophore was chosen as the EO active unit for construction of all dendritic chromophores in this study because of its robustness as well as its relatively large β value.[28−30] Thin-film composites of the dendritic compounds as well as FTC dispersed into amorphous polycarbonate (APC) were deposited atop ITO-coated glass substrates and evaluated for differences in EO activity. The dynamic behavior of EO response was observed using an in situ pole-and-probe, single-beam polarization interferometry reflection apparatus. Signal decay times were employed to estimate the activation energies associated with relaxation of the dipolar chromophore lattice. The effect of binding geometry and tether group composition on EO behavior was thus investigated.

Experimental Section

Detailed procedures for the synthesis as well as spectrometric characterization of compounds reported can be found in the accompanying Supporting Information.

(13) Ma, H.; Chen, B.; Sassa, T.; Dalton, L. R.; Jen, A. K.-Y. *J. Am. Chem. Soc.* **2001**, *123*, 986−987.
(14) Luo, J.; Ma, H.; Haller, M.; Jen, A. K.-Y.; Barto, R. R. *Chem. Commun.* **2002**, 888−889.
(15) Chasse, T. L.; Sachdeva, R.; Li., Q.; Petrie, R. J.; Gorman, C. B. *J. Am. Chem. Soc.* **2003**, *125*, 8250−8254.
(16) Furuta, P.; Frechet, J. M. J. *J. Am. Chem. Soc.* **2003**, *125*, 13173−13181
(17) Frechet, J. M. J.; Hawker, C. J.; Gitsov, I.; Leon, J. W. *J. Mater. Sci.-Pure Appl. Chem.* **1996**, *A33* (10), 1399−1425.
(18) Gopalan, P.; Katz, H. E.; McGee, D. J.; Erben, C.; Zielinski, T.; Bousquet, D.; Muller, D.; Grazul, J.; Olsson, Y. *J. Am. Chem. Soc.* **2004**, *126* (6), 1741−1747.
(19) Cha, S. W.; Choi, D. H.; Jin, J.-I. *Adv. Funct. Mater.* **2001**, *11* (5), 355−360.
(20) Breitung, E. M.; Shu, C.-F.; McMahon, R. J. *J. Am. Chem. Soc.* **2000**, *122*, 1154−1160.
(21) Varanasi, P. R.; Jen, A. K.-Y.; Chandrasekhar, A. J.; Namboothiri, I. N. N.; Rathna, A. *J. Am. Chem. Soc.* **1996**, *118*, 12443−12448.
(22) Albert, I. D. L.; Marks, T. J.; Ratner, M. A. *J. Am. Chem. Soc.* **1997**, *119*, 6575−6582.
(23) He, M. Q.; Leslie, T. M.; Sinicropi, J. A. *Chem. Mater.* **2002**, *14*, 4662−4668.
(24) Wu, X.; Wu, J.; Jen, A. K.-Y. *J. Am. Chem. Soc.* **1999**, *121*, 472−473.
(25) Bai, Y.; Song, N.; Gao, J. P.; Yu, G.; Sun, X.; Wang, X.; Wang, Z. Y. *J. Am. Chem. Soc.* **2005**, *127*, 2060−2061.
(26) Luo, J.; Haller, M.; Ma, H.; Liu, S.; Kim, T.-D.; Tian, Y.; Chen, B.; Jang, S.-H.; Dalton, L. R.; Jen, A. K-Y. *J. Phys. Chem. B* **2004**, *108*, 8523−8530.
(27) Ma, H.; Luo, J.; Kang, S. H.; Wong, S.; Kang, J. W.; Jen, A. K.-Y.; Barto, R.; Frank, C. W. *Macromol. Rapid Commun.* **2004**, *25*, 1667−1673.
(28) Breitung, E. M.; Shu, C.-F.; McMahon, R. J. *J. Am. Chem. Soc.* **2000**, *122*, 1154−1160.
(29) Varanasi, P. R.; Jen, A. K.-Y.; Chandrasekhar, J.; Namboothiri, I. N. N.; Rathna, A. *J. Am. Chem. Soc.* **1996**, *118*, 12443−12448.
(30) Albert, I. D. L.; Marks, T. J.; Ratner, M. A. *J. Am. Chem. Soc.* **1997**, *119*, 6575−6582.

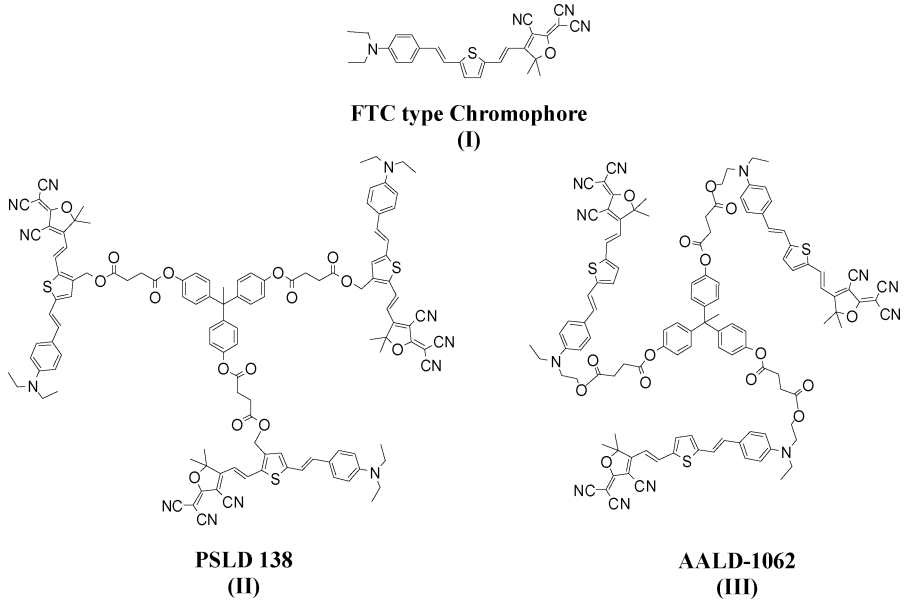

Figure 1. Free chromophore FTC (I), side-on dendritic chromophore (PSLD-138, II), and end-on dendritic chromophore (AALD-1062, III).

Thin-Film Fabrication for EO Study. Each dendritic chromophore was mixed with solid APC (6.14×10^{19} chromophore active molecules in 0.09 g of APC). The solid components were then dissolved into cyclopentanone (8% total solid weight). The solutions were stirred, filtered, and then spin-cast onto ITO-coated glass slides. Film thicknesses were measured to be 2.2−2.5 μm using a surface profilometer (KOSAKA, ET-3000). Gold was then deposited at the surface of the polymer−composite film to create both a reflective surface for measurement and an electrode for application of poling and modulating fields.

Real Time Pole and Probe Measurement of EO Effect. This method is a modification of the standard reflection technique used for measuring EO effects in thin films and calculating corresponding r_{33} values. For standard EO measurement the film was contact-poled and an ac voltage (10 V_{rms} at 1 kHz) was applied to the sample.[31] The modulated signal intensity (I_m) was simultaneously monitored. The linear EO coefficient r_{33} is directly proportional to I_m/I_c and was calculated using

$$r_{33} = \frac{3\lambda I_m}{4\pi V_m I_c n^2} \frac{(n^2 - \sin^2\theta)^{1/2}}{\sin^2\theta} \propto I_m/I_c \qquad (3)$$

In this equation, n is the refractive index at the probe beam wavelength ($\lambda = 1300$ nm), I_m is the amplitude of EO modulation, V_m is the ac voltage applied, and I_c is the intensity of incident light where the phase retardation between T_E and T_M is 90°.

dc biased or in situ measurements were performed by mounting the sample on a hot stage and applying a combination of a constant dc poling field (adjustable) and an ac modulating field, as represented by

$$V(t) = V_{dc} + V_0 \sin \omega t \qquad (4)$$

This method allows for simultaneous poling and probing of the sample while monitoring sample temperature and current flow.

Results and Discussion

The first two dendrimers (Figure 1) were based on a 1,1,1-tris(succinic acid phenyl ester)ethane core. This core incorporated a relatively short, inflexible, succinic acid ester, chromophore−core tether group.

Synthesis of the side-on EO-active moiety (6) began by Horner-Emmons olefination of (4-bromo-2-thienylmethyl)-phosphonate with aldehyde **1** to produce donor-bridge **2**. To create an attachment point, a low-temperature kinetic formylation reaction was used to produce aldehyde **3**. The aldehyde was reduced quantitatively to give 3-hydroxymethylene-substituted donor-bridge **4**. Product **4** was then formylated once again to give structure **5**. Knoevenagel condensation of the 2-cyanomethylene-3-cyano-4,5,5-trimethyl-2,5-dihydrofuran (TCF) acceptor to aldehyde **5** was performed to yield chromophore **6**, as a copper-like solid.[32,33] The 3-hydroxymethylene unit in chromophore **6** was then used to ring-open succinic anhydride. This reaction produced the carboxylic acid-functionalized chromophore **7**. Molecule **7** was then attached to 1,1,1-tris(4-hydroxy-phenyl)ethane to create the side-on dendritic chromophore PSLD-138 (II, Scheme 1).

Synthesis of the end-on type EO-active moiety (AALD-1062, compound III), proceeded in an analogous manner. The only variation was the creation of an attachment point on the donor side of the molecule rather than the bridge.

UV−visible absorption spectroscopy revealed that side-on compound II had a λ_{max} of 672 nm in chloroform solution and 655 nm in an APC film. This was very similar to FTC (I), which exhibited a λ_{max} of 672 nm in chloroform and 659 nm in APC film. End-on compound III showed a λ_{max} of 635 nm in chloroform and 627 nm in APC. This trend was also observed through cyclic voltametry analysis. Free FTC records a HOMO−LUMO energy gap $E_g = 1.529$ eV, while the dendritic chromophores II and III were found to exhibit $E_g = 1.503$ eV and $E_g = 1.606$ eV, respectively. The largest energy gap was displayed by end-on compound III while

(31) Michelotti, F.; Toussare, E.; Levenson, R.; Liang, J.; Zyss, J. *J. Appl. Phys.* **1995**, *80*, 1773−1778.
(32) Briers, D.; Koeckelberghs, G.; Picard, I.; Verbiest, T.; Persoons, A.; Samyn, C. *Macromol. Rapid Commun.* **2003**, *24*, 841−846.
(33) Zhang, C.; Wang, C.; Yang, J.; Dalton, L. R.; Sun, G.; Zhang, H.; Steier, W. H. *Macromolecules* **2001**, *34*, 235−243.

Scheme 1. Synthesis of Side-on Dendritic Chromophore PSLD-138 (II)[a]

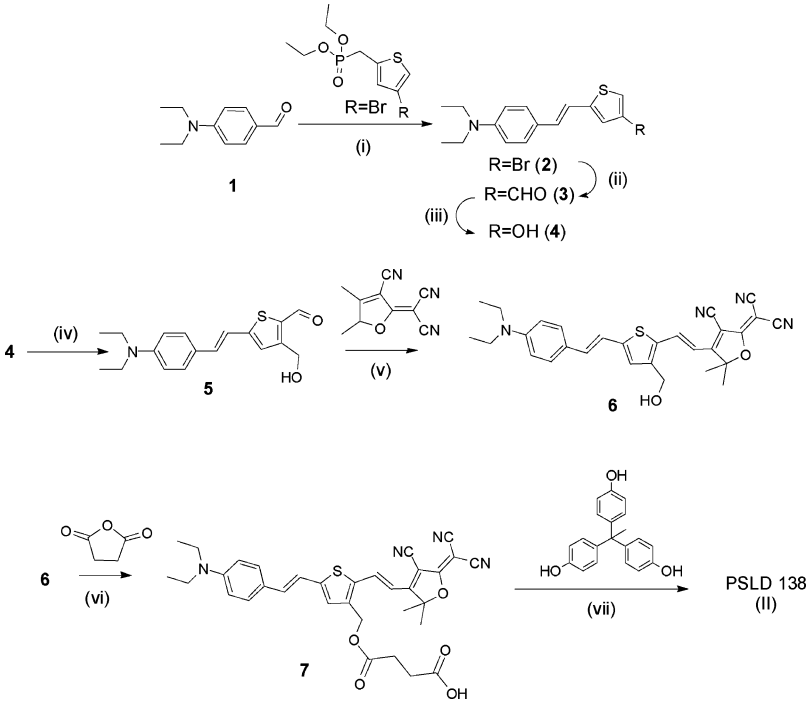

[a] Conditions: (i) ^{t}BuOK, THF, RT overnight, 90%; (ii) (a) *n*-BuLi, Et_2O −78 °C, 3 h; (b) DMF, RT, 18 h, 67%; (iii) $NaBH_4$/NaOH, MeOH/THF 0 °C−RT, quant.; (iv) (a) *n*-BuLi, THF, −78 °C, 3 h (b) DMF, RT, 18 h, 87%; (v) NH_4OAc/EtOH, 50 °C, 12 h (80%); (vi) DMAP, Py, DCM, RT, 6 h, 96%; (vii) DCC/DPTS, THF/DCM, RT, 24 h, 88%.

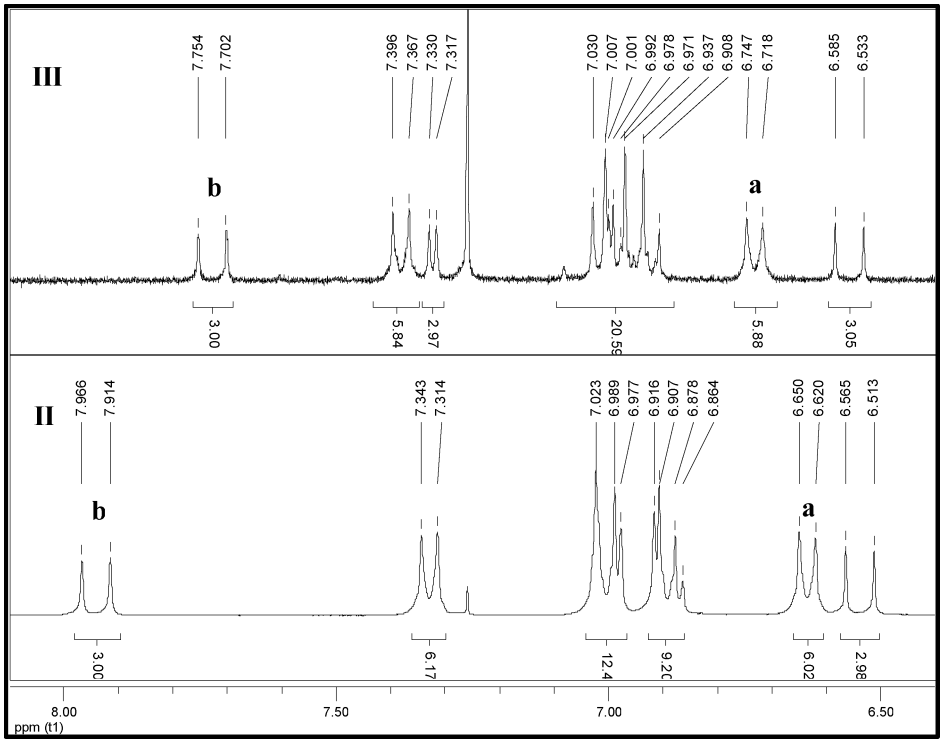

Figure 2. Aromatic region of ^{1}H NMR spectra of dendritic chromophores II and III.

side-on compound II displayed an energy gap similar to FTC. This difference can be understood by the presence of the electron-withdrawing ester group at different sites on the dipolar, conjugated system. Such an explanation was supported by ^{1}H NMR data (Figure 2). Doublet b (J_{H-H} = 15.5 Hz, trans C═C, 1H) can be assigned to vinylic protons closest to the chromophore electron-accepting moiety. These proton resonances exhibit a substantial downfield shift for side-on compound II. This shift is caused by a reduction of electron density at this site effected by the proximity of the ester tether group. Doublet a (J_{H-H} = 8.3 Hz, phenyl, 2H), was assigned to phenyl ring protons closest to the amine electron-donor portion of the chromophore. Doublet a shows a relative downfield shift for protons in this position on end-on compound III. This shift results from attachment of the ester tether group close to the amine donor, reducing electron

density at this site. The end-on attached system can be expected to be affected to a greater extent due to more effective communication between the nonbonding nitrogen lone pair and π^* of the ester. No other pronounced shift differences were observed in proton resonances between dendritic EO-active moieties. These specific differences in ^{1}H NMR spectra support the hypothesis that observed differences in optical E_g can be attributed largely to intramolecular effects rather than differing external interactions.

Variable angle spectroscopic ellipsometry measurements were performed on APC films containing FTC and dendritic compounds II and III (6.14×10^{19} chromophore active molecules in 0.09 g of APC). These data were used in combination with the absorption spectra of each film to accurately determine the real and imaginary part of refractive index at 1300 nm. With use of consistent measurement conditions, these samples containing FTC, side-on compound II, and end-on compound III displayed refractive indices of 1.68, 1.64, and 1.62, respectively. The larger refractive index displayed by samples containing free chromophore FTC relative to samples containing dendritic compounds II and III is consistent with a greater dielectric constant and larger first-order (linear) susceptibility. Due to a greater freedom of motion, bulk linear polarization is more easily induced in samples containing free chromophore FTC. Consistently, films containing side-on compound II display a higher refractive index than is recorded for samples containing end-on compound III. This refractive index data was then used for calculation of the EO coefficient.

Melting and glass transition temperatures were obtained for pure samples of the EO materials by differential scanning calorimetry. FTC displayed a melting and probable decomposition point at 242 °C, but showed no T_g. Dendritic chromophores II and III displayed almost identical T_g of 110 °C, regardless of the difference in the binding mode of the chromophore. Additionally, measurements of a thermally stimulated flowing current were performed using APC films containing comparable loading of the active materials (concentration noted above). This experiment was used to determine the temperature at which an abrupt spike in current was observed under applied dc voltage. This "transition temperature" (T_{tr}) can be used to help determine the optimum poling temperature for the EO experiments. The values of T_{tr} can be expected to correlate closely with the temperature required for an abrupt increase in degree of molecular freedom within the host matrix corresponding to energy required to overcome intermolecular interactions such as van der Waals forces. This T_{tr} is also an indication of proximity to the material dielectric breakdown point for a given temperature and electric field. The lowest temperature transition occurred for the sample containing FTC at 129 °C, followed by the sample containing end-on III at 158 °C, and then the highest by the sample of side-on II at 163 °C.

For the study of electro-optic activity, an equal number (concentrations noted previously) of active units (EO-active moieties) of pure materials FTC, succinic acid ester tether-based dendritic chromophores side-on II and end-on III were dissolved into amorphous polycarbonate (APC). To observe optimized EO coefficients as well as dynamic behavior, a real-time pole and probe modification to the simple reflection setup was used. Under a poling field of 70 V/μm, FTC demonstrated the highest average r_{33} (≈25 pm/V) of the three, while samples containing side-on II and end-on III displayed lower average r_{33} values of ≈9 and ≈5 pm/V, respectively.

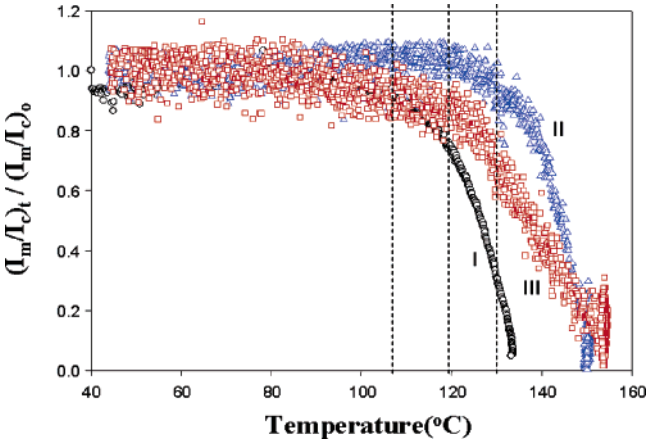

Figure 3. Thermally induced EO signal decay transitions for APC films containing side-on (II) and end-on (III) dendritic chromophores as well as FTC (I).

For the purpose of evaluating the temperature at which dipolar relaxation or loss of EO signal is initiated, a dynamic, thermally induced relaxation experiment was performed. Fresh films of dendrimers II and III as well as FTC in APC were poled to reach their respective maximum EO signal as previously described. The samples were cooled with continued application of the dc poling field. The poling field was then removed and a temperature ramp (5 °C/min) was initiated while observing I_m/I_c. The resulting data traces were normalized and plotted against one another. Data corresponding to thin-film APC composites of FTC (I), succinic acid-based side-on (II), and end-on (III) are shown in Figure 3.

The data show that the highest temperature was required to initiate abrupt dipolar relaxation in the side-on attached dendritic chromophore II samples (approximately 130 °C). A temperature of approximately 110 °C was required to initiate fast relaxation of a sample containing FTC, and 120 °C was required for samples of end-on III. This suggested that the activation energy required for dipole relaxation and thus randomization was smaller for the end-on than for the side-on dendrimer samples.

An isothermal decay study at 105 °C was also performed using APC samples containing FTC, and each of the two succinic acid-based dendritic chromophores (Figure 4).

Conditions similar to those that could be encountered by a working EO device were approximated by this experiment. After poling, the samples were cooled to 105 °C, and the EO signal decay was monitored with respect to time. The data obtained shows that the dendrimer systems indeed demonstrate much more thermally stable EO properties than the simple guest−host system exemplified by FTC/APC composites. The sample composed of FTC in APC shows a fast and dramatic decay whereas the decay rate is greatly retarded for samples composed of dendritic chromophores in APC.

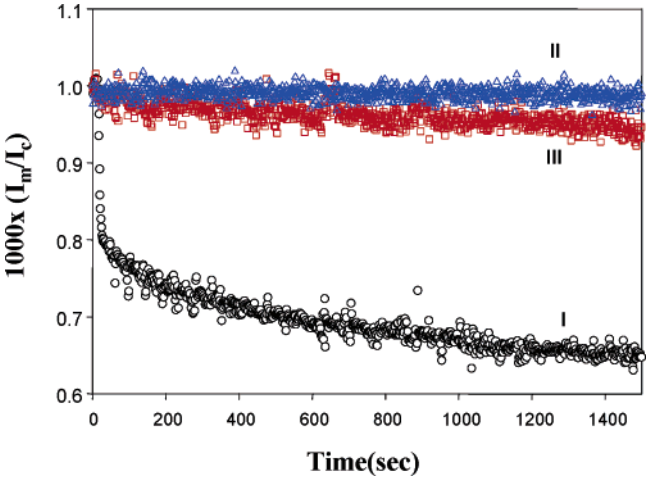

Figure 4. Isothermal EO stability data for APC films containing FTC (I), succinic acid tether-based side-on (II), and end-on (III). * Temperature: 105 °C.

Noting the greatly lowered EO activity of the succinic acid tether group-based dendritic chromophores compared to their free chromophore counterpart, a longer, more flexible tether unit, seemed desirable. To realize this idea, two new dendritic chromophores were designed and synthesized based on a 1,1,1-tris(6-phenoxy-hexanoic acid ester)ethane core.

Synthesis of PSLD-31 (side-on dendrimer IV) and AALD-1104 (end-on dendrimer V) is illustrated in Scheme 2.

Esterification of 6-bromo-1-hexanoic acid (**8**) was performed overnight using methanol and catalytic sulfuric acid to yield 6-bromo-1-hexanoic acid methyl ester (**9**). The standard Frechet-type tri-phenol core, (1,1,1-tris(4-hydroxyphenyl)ethane), was then trifunctionalized with **9** using sodium hydride under Williamson conditions to produce **10**. This tri-ester core was then saponified to produce 1,1,1-tris-(6-phenoxy-hexanoic acid)ethane (**11**), a compound bearing three carboxylic acid-terminated, highly flexible aliphatic tether groups. Side-on type chromophore (**6**) bearing a center-affixed hydroxyl group, identical to that of the active moiety in side-on compound II, was then attached to each tether group again under mild esterification conditions to yield hexanoic acid ester (HE) tether group-based, side-on, first generation dendrimer PSLD-31 (IV). A similar procedure was followed in preparation of the HE-end-on, first generation dendrimer AALD-1104 (V). Both dendritic materials were obtained as metallic blue solids. Side-on IV exhibited a $\lambda_{max} = 679$ nm in $CHCl_3$, somewhat red-shifted relative to a $\lambda_{max} = 640$ nm for end-on V. These data were consistent with the previous succinate ester-based dendrimers. Both side-on IV and end-on V were dissolved into solutions of

Scheme 2. Synthetic Scheme for Hexanoic Acid Ester-Based Dendritic Chromophores IV and V[a]

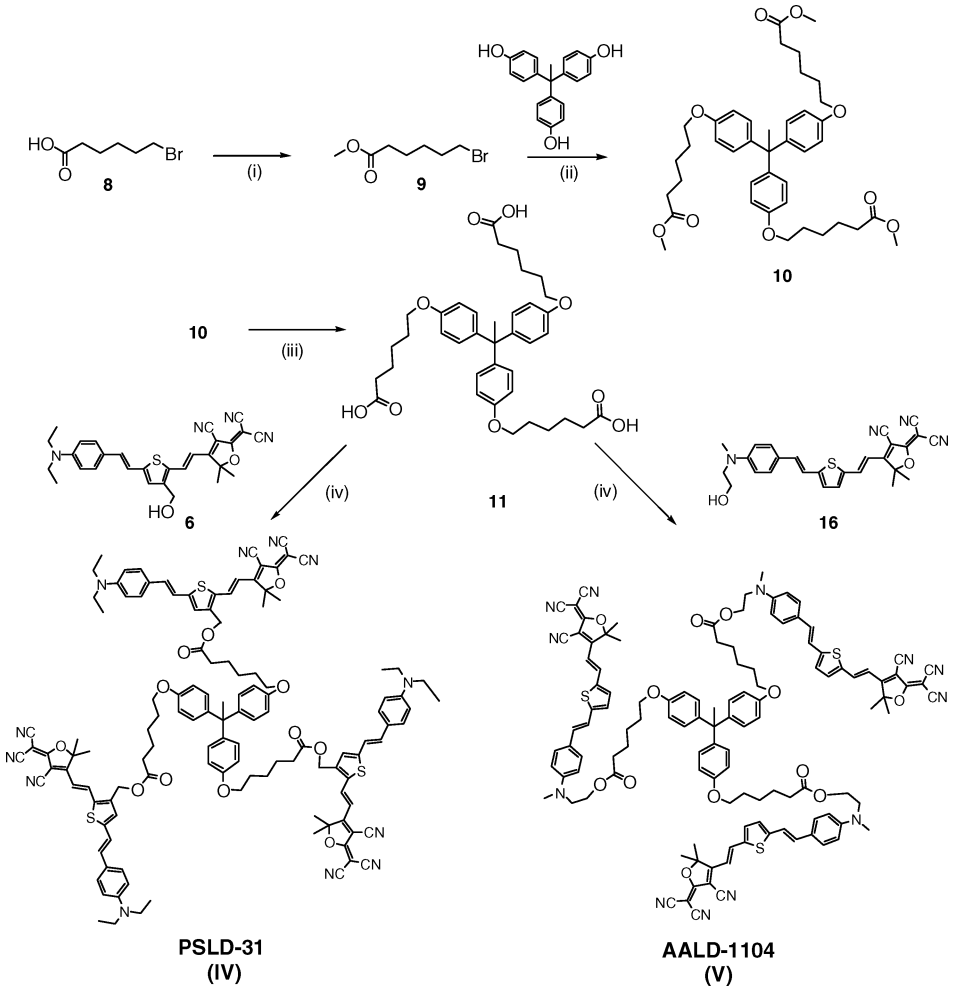

[a] Conditions: (i) H_2SO_4, MeOH, overnight, quant.; (ii) NaH, DMF, 90 °C, 12 h, >99%; (iii) NaOH, acetone, 5 h, 89%; (iv) DCC, DPTS, CH_2Cl_2, 24 h, RT, 25−68%.

Table 1. Average and Maximum r_{33} Values for Succinate Dendritic Chromophores II and III, Hexanoic Acid Ester Dendritic Chromophores (IV and V), and Free Chromophore FTC, Doped into APC

compound	spacer	E_p (V/μm)	T_g (°C)	time (min)	max r_{33} (pm/V)	ave. r_{33} (pm/V)[a]
side-on II	diester	70	110	15	10	9
end-on III	diester	70	110	15	7	5
side-on IV	HE	70	125	15	35	27
end-on V	HE	70	90	15	26	20
FTC		70		15	30	25

[a] Average value of five fresh samples poled under identical conditions.

APC and cyclopentanone so that each formulation contained an equal number of active molecules with respect to weight of APC, in the same concentration as above. Thin-film samples were then fabricated using the new dendrimers.

Thermally stimulated current (TSC) transition temperatures (T_{tr}) were observed as before. Unlike the previous succinate ester-based dendritic chromophores II and III, the new compounds IV and V displayed significantly different T_{tr} values. Samples composed of side-on dendritic chromophore IV in APC show a T_{tr} of approximately 120 °C. End-on V in APC displayed T_{tr} of approximately 110 °C. As before, higher poling temperatures were required for side-on IV-based samples under the same poling field. Thermal analysis by DSC also revealed a lower T_g of 90 °C for pure end-on compound V while pure side-on IV displayed a T_g of 125 °C.

Observation of equilibrium EO values revealed that, under identical experimental conditions, differences in r_{33} between side-on and end-on geometries were small, but they were consistent over multiple samples. The average r_{33} value obtained for samples of side-on IV under a dc poling field of 70 V/μm was 27 pm/V. The average r_{33} for end-on V was 20 pm/V. EO properties are tabulated in Table 1; a maximum r_{33} value is shown in addition to an average determined from the values of five freshly poled samples in order to illustrate approximate range in r_{33}. The values obtained using hexanoic acid tether-based dendritic chromophores IV and V represent a significant improvement over previous succinic acid tether-based dendritic chromophores II and III.

Dynamic thermal decay experiments were again performed using samples of the new materials. The resulting data show that a higher temperature was again required to initiate abrupt dipolar relaxation in the side-on attached dendrimer IV samples. Somewhat lower temperatures were required to initiate fast decay in samples of dendrimers IV and V than in samples containing dendrimers II and III. This behavior was expected due to the more aliphatic nature (longer chain length and increased flexibility) of the hexanoic acid ester tether in IV and V. A temperature of approximately 108 °C was required to initiate fast relaxation of a sample containing end-on V, and 114 °C was required for samples of side-on IV. Again the side-on type compound consistently displayed a more thermally stable EO signal (Figure 5).

To more precisely compare average activation energies for initiation of dipolar relaxation between the side-on and end-on binding geometries, EO decay curves of the two new

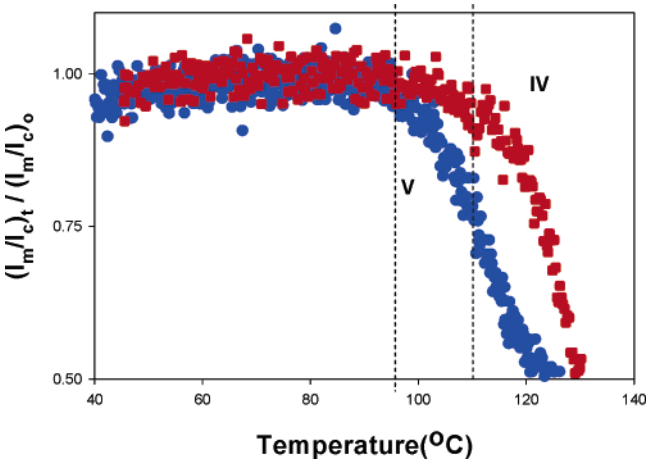

Figure 5. Thermally induced EO signal decay transitions for APC samples containing hexanoic acid tether-based dendritic chromophores IV and V heated at a ramp rate of 10 °C/min.

hexanoic acid tether group-based compounds were recorded at various elevated temperatures, normalized, and plotted. Data were gathered for samples containing dendritic chromophores IV and V at experimental temperatures of 109, 114, and 119 °C. These data were then analyzed by curve fitting, using the Kohlrausch−Williams−Watts (KWW) stretched exponential function.

$$(I_m/I_c)_t = (I_m/I_c)_\infty + \Delta(I_m/I_c)\exp(-t/\tau)^\beta \qquad (5)$$

where τ represents relaxation time and β represents a stretching parameter. The KWW function yields an average relaxation time $\langle\tau\rangle$ given by[34]

$$\langle\tau\rangle = (\tau/\beta)\Gamma(1/\beta) \qquad (6)$$

Activation energies (kcal/mol) for dipolar relaxation were then estimated from a linear plot of log $\langle\tau\rangle$ vs $1/T$. Isothermal decay data for APC samples containing compounds IV and V are depicted in Figure 6.

Comparison of average relaxation times $\langle\tau\rangle$ reveals that side-on IV exhibits much larger average activation energies (303 kcal/mol compared to 125 kcal/mol, Table 2). These data emphasize the point that the side-on chromophore attachment geometry provides improved thermal EO signal stability when compared with the end-on attached arrangement.

As an amorphous polymeric film is heated near its glass transition, molecular motion rates may be expected to increase abruptly by nearly 10 orders of magnitude.[35] This high rate of molecular motion promotes both ordering in the presence of an electric field and relaxation to a preferred state without. The energy required to cause this increase in average molecular motion depends on many factors. These factors may include polymer main chain rigidity, degree of branching, free volume, chromophore binding mode, and chromophore electrostatic interactions.[35−37] Upon poling, the

(34) Lindsey, C. P.; Patterson, G. D. *J. Chem. Phys.* **1980**, *73* (7), 3348−3357.
(35) Ediger, M. D. *Annu. Rev. Phys. Chem.* **2000**, *51*, 99−128.
(36) Bahar, I.; Erman, B.; Fytas, G.; Steffen, W. *Macromolecules* **1994**, *27*, 5200−5205.
(37) De Gennes, P. G. *J. Chem. Phys.* **1971**, *55* (2), 572−579.

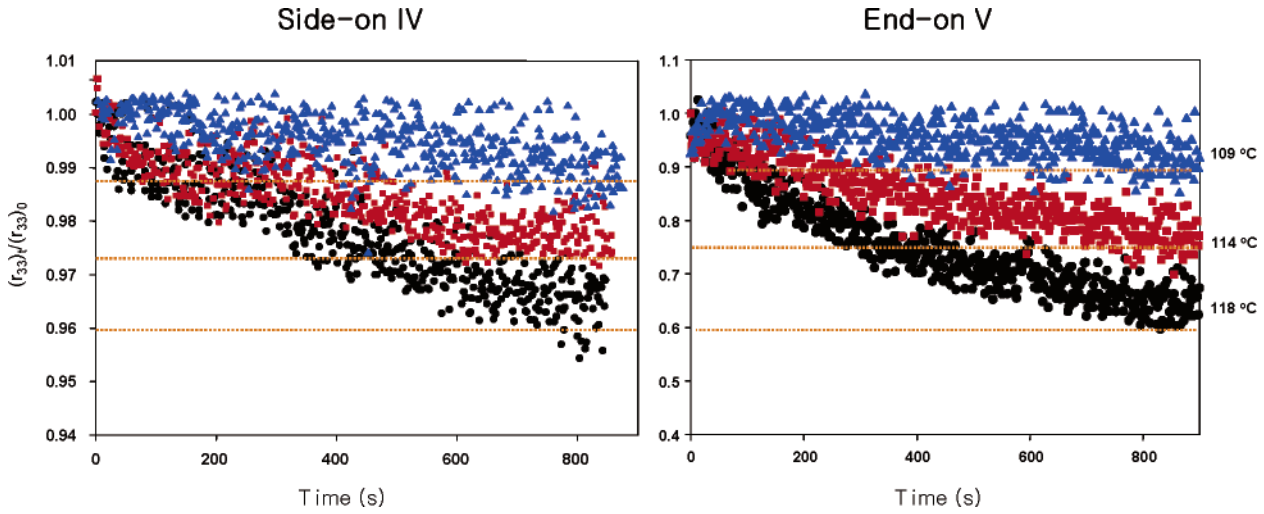

Figure 6. Data plots depicting EO decay of poled APC samples containing dendritic chromophores IV and V heated at constant temperatures of 109, 114, and 118 °C.

Table 2. Isothermal Decay Data: Relaxation Time (τ), Average Relaxation Time ($\langle\tau\rangle$), Stretching Parameters (β), and Activation Energies (E_a), for Dendritic Chromophores IV and V

	end-on V			side-on IV		
temp	τ (s)	$\langle\tau\rangle$ (s)	b	τ (s)	$\langle\tau\rangle$ (s)	b
118 °C	47.39	817.54	0.337	133.37	666.57	0.3506
114 °C	67.66	1369.50	0.300	454.55	14354.25	0.227
109 °C	409.33	32669.02	0.256	2327.21	6037700.72	0.150
E_a (kcal/mol)		124.57			302.84	

dipolar order induced within the guest−host, dipolar chromophore system induces intra- and intermolecular strain. The nature and magnitude of this strain is strongly dependent on chromophore shape and the nature of the interaction of the dipolar unit with its surroundings.

Conclusions

Four novel dendritic chromophores were synthesized. These dendritic EO-active materials were dispersed into APC and tested as thin-film composites using a real-time, in situ pole-and-probe EO measurement apparatus. The results demonstrate a dependence of EO behavior on chromophore tethering orientation. The side-on type dendritic chromophore showed greater thermal stability (higher activation energy for dipolar randomization) than the end-on type. The differences in average r_{33} between side-on and end-on geometries were rather small but consistent. EO behavior was shown to depend heavily on the length and rigidity of the moieties used to covalently anchor the chromophore to the inert host or core. A nearly 3-fold enhancement in EO coefficient was noted when the short di-ester tether group was replaced by a longer, more aliphatic system. Changes in tether group rigidity might be expected to also affect the magnitude of the r_{33} difference between side-on and end-on attachment geometry but the data obtained suggest that these effects are small. The major differences are observed in thermal stability data. The hexanoic acid-based molecules IV and V displayed r_{33} values that were very comparable to those of FTC while maintaining much improved thermal EO stability. All four dendrimer systems exhibited much slower thermally induced EO signal decay rates as compared to free chromophore FTC. This study demonstrates the importance of seemingly subtle design changes in the nanoscale architecture of dendritic chromophore systems for second-order nonlinear optics. It also suggests intelligently designed dendritic EO chromophores as promising candidates for further development.

In future experiments we seek to further explore the use of these dendritic effects in the rational design of new materials with greatly amplified EO coefficients. Incorporation of chromophores with enhanced hyperpolarizabilities is in progress. In addition, amplification of the dendrimer site-isolation effect can be achieved through the addition of bulky second generation dendrons to the outer periphery, thereby increasing the degree of chromophore encapsulation. The use of an optically inert host polymer matrix inherently reduces EO material performance through restrictive effects, compatibility problems, and reduced active chromophore content per unit volume. An attractive goal and potential improvement may be found in polymer-free, all dendrimer thin films. In addition to the high thermal stability of EO effects demonstrated by dendritic chromophore architectures, lattice hardening chemistry can be envisioned to further improve thermal properties.

Acknowledgment. The authors thank the Robinson and Jen research groups at the University of Washington. Financial support for the project was provided by The Lumera Corporation, The NSF Science and Technology Center MDITR-(DMR0120967), and NSF-(DMR0092380), U.S. Air Force AFSOR-(F49620-03-1-0110-P000), and the DARPA-MORPH program (N)))14-04-10094).

Supporting Information Available: Detailed procedures for the synthesis as well as spectrometric characterization of the dendritic chromophore compounds reported. This material is available free of charge via the Internet at http://pubs.acs.org.

CM0517420